Peter Benner Matthias Voigt

A Structured Pseudospectral Method for $\mathcal{H}_\infty$-Norm Computation of Large-Scale Descriptor Systems

Max Planck Institute Magdeburg Preprints

MPIMD/12-10 **May 3, 2012**

Impressum:

Max Planck Institute for Dynamics of Complex Technical Systems, Magdeburg

Publisher:
Max Planck Institute for Dynamics of Complex Technical Systems

Address:
Max Planck Institute for Dynamics of Complex Technical Systems
Sandtorstr. 1
39106 Magdeburg

www.mpi-magdeburg.mpg.de/preprints

A STRUCTURED PSEUDOSPECTRAL METHOD FOR $\mathcal{H}_\infty$-NORM COMPUTATION OF LARGE-SCALE DESCRIPTOR SYSTEMS

PETER BENNER* AND MATTHIAS VOIGT*

Abstract. In this paper we discuss the problem of computing the $\mathcal{H}_\infty$-norms of transfer functions associated to large-scale descriptor systems. We exploit the relationship between the $\mathcal{H}_\infty$-norm and the structured complex stability radius of the corresponding system pencil. To compute the structured stability radius we consider so-called structured pseudospectra. Namely, we have to find the pseudospectrum touching the imaginary axis. Therefore, we set up an iteration over the real part of the rightmost pseudoeigenvalue. For that we use a new fast iterative scheme which is based on certain rank-1 perturbations of the system pencil. Finally, we analyze the performance of our algorithm by using real-world examples.

Key words. Descriptor systems, $\mathcal{H}_\infty$ control, iterative methods, pseudospectra, sparse matrices, stability of linear systems.

1. Introduction and Preliminaries. In this paper we consider linear time-invariant descriptor systems of the form

$$\begin{aligned} E\dot{x}(t) &= Ax(t) + Bu(t), \\ y(t) &= Cx(t), \end{aligned} \tag{1.1}$$

where E, $A \in \mathbb{R}^{n\times n}$, $B \in \mathbb{R}^{n\times m}$, $C \in \mathbb{R}^{p\times n}$, $x(t) \in \mathbb{R}^n$ is the descriptor vector, $u(t) \in \mathbb{R}^m$ is the input vector, and $y(t) \in \mathbb{R}^p$ is the output vector. Sometimes we will denote such a system by $\Sigma = (\lambda E - A, B, C)$. Throughout this paper we assume that $\lambda E - A$ is a *regular* matrix pencil, i.e., $\det(\lambda E - A) \not\equiv 0$. Furthermore we assume that all involved matrices are large and sparse with m, $p \ll n$. We will call a descriptor system stable if $\Lambda_\mathrm{f}(E, A) \subset \mathbb{C}^- := \{s \in \mathbb{C} : \mathrm{Re}\,(s) < 0\}$, where $\Lambda_\mathrm{f}(E, A)$ is the set of all finite eigenvalues of $\lambda E - A$.

Instead of working in the time domain we often turn to the Laplace domain. By taking the Laplace transforms of both equations in (1.1) and assuming $Ex(0) = 0$ we obtain the transfer function [10]

$$G(s) = C(sE - A)^{-1}B. \tag{1.2}$$

We call $G(s)$ *asymptotically stable* if all its *finite* poles are located in the open left half-plane, i.e., $\Pi_\mathrm{f}(E, A, B, C) \subset \mathbb{C}^-$, where $\Pi_\mathrm{f}(E, A, B, C)$ denotes the set of all finite poles of $G(s)$. For brevity we will just call such a transfer function stable since we exclude poles on the imaginary axis. Furthermore, we call $G(s)$ *proper* if $\lim_{\omega\to\infty} \|G(\mathrm{i}\omega)\|_2 < \infty$, otherwise we call it *improper*. By $\mathcal{RH}_\infty^{p\times m}$ we denote the rational Banach space of all stable and proper functions of the form (1.2), see, e.g., [26]. For this space we define the $\mathcal{H}_\infty$*-norm*, given by

$$\|G\|_{\mathcal{H}_\infty} := \sup_{s\in\mathbb{C}^+} \sigma_{\max}(G(s)) = \sup_{\omega\in\mathbb{R}} \sigma_{\max}(G(\mathrm{i}\omega)),$$

with $\mathbb{C}^+ := \{s \in \mathbb{C} : \mathrm{Re}\,(s) > 0\}$ and the maximum singular value $\sigma_{\max}(\cdot)$. Our aim is to compute this norm value under the given assumptions.

Numerical methods for computing the $\mathcal{H}_\infty$-norm have been known for a long time. Most of them are based on relations between the $\mathcal{H}_\infty$-norm and the spectrum of certain

*Max Planck Institute for Dynamics of Complex Technical Systems, Sandtorstr. 1, 39106 Magdeburg, Germany (benner@mpi-magdeburg.mpg.de, voigtm@mpi-magdeburg.mpg.de).

Hamiltonian matrices or pencils. For an overview, we refer to the works [2–6]. We briefly summarize the most general result presented in [2]. Under some assumptions it holds that $\|G\|_{\mathcal{H}_\infty} < \gamma$ if and only if the *skew-Hamiltonian/Hamiltonian matrix pencil* [1]

$$\lambda\mathcal{S} - \mathcal{H}_\gamma = \lambda \begin{bmatrix} E & 0 \\ 0 & E^T \end{bmatrix} - \begin{bmatrix} A & \frac{1}{\gamma} BB^T \\ -\frac{1}{\gamma} C^T C & -A^T \end{bmatrix}$$

has no finite, purely imaginary eigenvalues. Based on that, the algorithm chooses an initial guess $\gamma < \|G\|_{\mathcal{H}_\infty}$ and iterates over γ in a suitable way until $\lambda\mathcal{S} - \mathcal{H}_\gamma$ has no finite, purely imaginary eigenvalues. This iteration can be implemented in a globally quadratically converging way. The drawback of the algorithm is the decision in each step whether there are purely imaginary eigenvalues. It is important to find *all* of them since otherwise the algorithm could fail. In [2] this issue was addressed by using a structure-preserving method for $\lambda\mathcal{S} - \mathcal{H}_\gamma$, which prevents the finite, purely imaginary eigenvalues to move off the imaginary axis as long as their pairwise distance is sufficiently large [1]. However, this method computes a full structured factorization of the pencil in each step. Due to its cubic complexity it is infeasible for large-scale problems. We could consider a closely related extended *even matrix pencil* and try to compute the desired eigenvalues close to a specified shift with the method presented in [17]. However, the question remains how to reliably compute *all* finite, purely imaginary eigenvalues. Another approach presented in [7, 8] uses the so-called bounded real lemma to estimate the $\mathcal{H}_\infty$-norm of a discrete-time state-space system which is required to be given in a minimal realization [10]. This algorithm checks a sequence of linear matrix inequalities for feasibility. This is done by deciding if a so-called Chandrasekhar iteration converges. However, this test lacks of reliability, in particular if the iterates are approaching the $\mathcal{H}_\infty$-norm. Hence, only an estimation of the norm value can be given by this algorithm. Therefore, in this paper we use another approach based on pseudospectra.

Our paper is structured as follows. In Section 2 we introduce the basic terminology and concepts that we will make use of in this work. In Section 3 we derive the mathematical basis of our algorithm. In particular, we describe how to compute the so-called structured pseudospectral abscissa of a transfer function which is the key ingredient of this paper. Finally, in Section 4 we present a study of numerical examples. We analyse the behavior of our method and state drawbacks and limitations.

2. Mathematical Preliminaries and Applications. In the following we need the following concepts and terminology. A regular matrix pencil $\lambda E - A$ can be reduced to *Weierstraß canonical form* [15]

$$E = W \begin{bmatrix} I_{n_\mathrm{f}} & 0 \\ 0 & N \end{bmatrix} T, \quad A = W \begin{bmatrix} J & 0 \\ 0 & I_{n_\infty} \end{bmatrix} T, \tag{2.1}$$

where W and T are nonsingular, I_k is an identity matrix of order k, J and N are in Jordan canonical form and N is nilpotent with index of nilpotency ν. The number ν is also called the *algebraic index* of the descriptor system (1.1) and n_f and n_∞ are the dimensions of the deflating subspaces of $\lambda E - A$ corresponding to the finite and infinite eigenvalues, respectively. We say that a finite or infinite eigenvalue is *defective*, if one of the corresponding Jordan blocks in J or N is larger than one. By using the transformation matrices W and T we can also write B and C as

$$B = W^{-1} \begin{bmatrix} B_1 \\ B_2 \end{bmatrix}, \quad C = \begin{bmatrix} C_1 & C_2 \end{bmatrix} T^{-1},$$

to obtain an equivalent descriptor system.

Furthermore we need some controllability and observability concepts [10]. The descriptor system (1.1) is called

- *completely controllable*, if rank $\begin{bmatrix} \lambda E - A & B \end{bmatrix} = n$ for all $\lambda \in \mathbb{C}$ and furthermore rank $\begin{bmatrix} E & B \end{bmatrix} = n$;
- *completely observable*, if rank $\begin{bmatrix} \lambda E^T - A^T & C^T \end{bmatrix} = n$ for all $\lambda \in \mathbb{C}$ and furthermore rank $\begin{bmatrix} E^T & C^T \end{bmatrix} = n$.

We can also define these concepts for single eigenvalues of $\lambda E - A$. A descriptor system (1.1) is called

- *controllable at* $\lambda \in \mathbb{C}$ if rank $\begin{bmatrix} \lambda E - A & B \end{bmatrix} = n$;
- *controllable at* $\lambda = \infty$ if rank $\begin{bmatrix} E & B \end{bmatrix} = n$;
- *observable* at $\lambda \in \mathbb{C}$ if rank $\begin{bmatrix} \lambda E^T - A^T & C^T \end{bmatrix} = n$;
- *observable* at $\lambda = \infty$ if rank $\begin{bmatrix} \lambda E^T & C^T \end{bmatrix} = n$;

otherwise it is called uncontrollable or unobservable at λ, respectively. Note, that in the above definition one can also consider each individual Jordan block of the Weierstraß canonical form separately in case of multiple eigenvalues. This is possible by considering the corresponding eigenvectors. Let x and y be right and left eigenvectors corresponding to a Jordan block in J or N of (2.1). Then

$$y^H \begin{bmatrix} \lambda E - A & B \end{bmatrix} = \begin{bmatrix} 0 & y^H B \end{bmatrix}, \quad x^H \begin{bmatrix} \lambda E^T - A^T & C^T \end{bmatrix} = \begin{bmatrix} 0 & x^H C^T \end{bmatrix}.$$

We say that such a Jordan block is controllable if $B^H y \neq 0$, and observable if $Cx \neq 0$, otherwise we call it uncontrollable or unobservable. We use this definition when talking about controllability and observability of eigenvalues.

A descriptor system $\Sigma = (\lambda E - A, B, C)$ which induces the transfer function $G(s) = C(sE - A)^{-1}B$ is called a *realization* of $G(s)$. Every rational function $G(s)$ admits such a descriptor system realization. A realization of $G(s)$ of the form (1.1) is called *minimal* if its order n is the smallest among all possible realizations. This is the case if and only if it is completely controllable and completely observable.

The $\mathcal{H}_\infty$-norm has several applications, for instance it is used in model order reduction as an error measure. Assume that

$$\begin{aligned} \tilde{E}\dot{\tilde{x}}(t) &= \tilde{A}\tilde{x}(t) + \tilde{B}u(t), \\ \tilde{y}(t) &= \tilde{C}\tilde{x}(t), \end{aligned} \tag{2.2}$$

with $\tilde{E}$, $\tilde{A} \in \mathbb{R}^{r\times r}$, $\tilde{B} \in \mathbb{R}^{r\times m}$, $\tilde{C} \in \mathbb{R}^{p\times r}$, reduced descriptor vector $\tilde{x}(t) \in \mathbb{R}^r$ and output vector $\tilde{y}(t) \in \mathbb{R}^p$ is a stable reduced-order model of (1.1). Then the transfer function of the error system is given by

$$G_{\mathrm{err}}(s) = \begin{bmatrix} C & -\tilde{C} \end{bmatrix} \left(s \begin{bmatrix} E & 0 \\ 0 & \tilde{E} \end{bmatrix} - \begin{bmatrix} A & 0 \\ 0 & \tilde{A} \end{bmatrix} \right)^{-1} \begin{bmatrix} B \\ \tilde{B} \end{bmatrix}.$$

The value of $\|G_{\mathrm{err}}\|_{\mathcal{H}_\infty}$ can be interpreted as the worst-case error when evaluating G_{err} in the frequency domain.

Another field of application can be found in robust control where the $\mathcal{H}_\infty$-norm takes the role of a robustness measure. Consider an output feedback controller $K \in \mathbb{R}^{m\times p}$ that stabilizes the system (1.1). This leads to the closed-loop dynamics

$$E\dot{x}(t) = A_K x(t) := (A + BKC)\, x(t).$$

In robust control we are interested in the robustness of the closed-loop systems with respect to perturbations in the controller K. In other words we want to know how

much we can maximally perturb K such that the perturbed closed-loop system is guaranteed to be stable. The perturbed closed-loop system is given by

$$E\dot{x}(t) = A_{K+\Delta}x(t) = (A_K + B\Delta C)\,x(t).$$

For stable systems (1.1) we define the numbers (we replace A_K by A for simplicity)

$$\begin{aligned} q_{\mathbb{C}}^{\mathrm{f}}(E,A,B,C) :&= \inf\left\{\|\Delta\|_2 : \Lambda_{\mathrm{f}}(E, A+B\Delta C)\cap \mathrm{i}\mathbb{R} \neq \emptyset \text{ with } \Delta\in\mathbb{C}^{m\times p}\right\},\\ q_{\mathbb{C}}^{\infty}(E,A,B,C) :&= \inf\left\{\|\Delta\|_2 : \Lambda_{\infty}(E, A+B\Delta C) \text{ with } \Delta\in\mathbb{C}^{m\times p}\right.\\ &\qquad\qquad \left.\text{has controllable and observable defective eigenvalues }\right\}, \end{aligned}$$

where $\Lambda_\infty(E,A)$ is the set of infinite eigenvalues of $\lambda E - A$ (counting multiplicity). Then we define the *structured complex stability radius of a matrix pencil* $\lambda E - A$ [13,14] by

$$q_{\mathbb{C}}(E,A,B,C) := \min\left\{q_{\mathbb{C}}^{\mathrm{f}}(E,A,B,C), q_{\mathbb{C}}^{\infty}(E,A,B,C)\right\}.$$

The value of $q_{\mathbb{C}}^{\mathrm{f}}(E,A,B,C)$ is the size of the smallest structured perturbation that makes the system unstable. The interpretation of $q_{\mathbb{C}}^{\infty}(E,A,B,C)$ is more involved. Defective infinite eigenvalues do not make the system unstable. However, if there are controllable and observable ones we can construct an arbitrarily small structured perturbation such that the system will be unstable. This means that systems with controllable and observable infinite eigenvalues are on the "boundary to instability".

It is desirable to make $q_{\mathbb{C}}(E,A,B,C)$ as large as possible in order to guarantee a very high robustness against perturbations in the controller. Later in this paper we show that for stable systems

$$q_{\mathbb{C}}(E,A,B,C) = \begin{cases} \frac{1}{\|G\|_{\mathcal{H}_\infty}} & \text{if } G \not\equiv 0,\\ \infty & \text{if } G \equiv 0, \end{cases}$$

so a high value of $q_{\mathbb{C}}(E,A,B,C)$ corresponds to a small $\mathcal{H}_\infty$-norm of the transfer function $G(s)$.

We also introduce the structured complex stability radius for a transfer function $G \in \mathcal{RH}_\infty^{p\times m}(\mathrm{i}\omega)$ which slightly differs from the one for matrix pencils. We define the numbers

$$\begin{aligned} r_{\mathbb{C}}^{\mathrm{f}}(E,A,B,C) :&= \inf\left\{\|\Delta\|_2 : \Pi_{\mathrm{f}}(E, A+B\Delta C, B, C)\cap \mathrm{i}\mathbb{R} \neq \emptyset \text{ with } \Delta\in\mathbb{C}^{m\times p}\right\},\\ r_{\mathbb{C}}^{\infty}(E,A,B,C) :&= \inf\left\{\|\Delta\|_2 : \Pi_{\infty}(E, A+B\Delta C, B, C) \neq \emptyset \text{ with } \Delta\in\mathbb{C}^{m\times p}\right\}\\ &= \inf\Big\{\|\Delta\|_2 : C\left(sE-(A+B\Delta C)\right)^{-1}B \text{ with } \Delta\in\mathbb{C}^{m\times p}\\ &\qquad\qquad \text{is improper}\Big\}, \end{aligned}$$

where $\Pi_\infty(E,A,B,C)$ is the set of infinite poles of $G(s)$. Then the *structured complex stability radius of a transfer function* $G(s)$ is defined by

$$r_{\mathbb{C}}(E,A,B,C) := \min\left\{r_{\mathbb{C}}^{\mathrm{f}}(E,A,B,C), r_{\mathbb{C}}^{\infty}(E,A,B,C)\right\}.$$

For stable or minimal descriptor systems we have that $q_{\mathbb{C}}^{\mathrm{f}}(E,A,B,C) = r_{\mathbb{C}}^{\mathrm{f}}(E,A,B,C)$ and $q_{\mathbb{C}}(E,A,B,C) = r_{\mathbb{C}}(E,A,B,C)$. However, $G \in \mathcal{RH}_\infty^{p\times m}(\mathrm{i}\omega)$ can also be realized by an unstable descriptor system when all unstable eigenvalues are uncontrollable or unobservable. In this case, the definitions of $q_{\mathbb{C}}^{\mathrm{f}}(E,A,B,C)$ and $q_{\mathbb{C}}(E,A,B,C)$ do not make sense whereas those of $r_{\mathbb{C}}^{\mathrm{f}}(E,A,B,C)$ and $r_{\mathbb{C}}(E,A,B,C)$ do. It is very important to well distinguish between these definitions.

3. Theoretical Framework. In this section we derive the theoretical basis of our algorithm. First of all we prove the relationship between the $\mathcal{H}_\infty$-norm and the structured complex stability radius.

LEMMA 3.1. *It holds that*

$$r_{\mathbb{C}}^{\infty}(E,A,B,C) = \begin{cases} \frac{1}{\lim\limits_{\omega\to\infty} \sigma_{\max}(G(\mathrm{i}\omega))} & \text{if } G \not\equiv 0, \\ \infty & \text{if } G \equiv 0. \end{cases}$$

Proof. If $G \equiv 0$, we cannot make the system improper by any structured perturbation, and therefore $r_{\mathbb{C}}^{\infty}(E,A,B,C) = \infty$. Consider the non-trivial case. W.l.o.g. we can assume that we have a minimal realization of a proper $G(s)$ given in Weierstraß canonical form, i.e.,

$$\Sigma = \left(\lambda \begin{bmatrix} I_{n_\mathrm{f}} & 0 \\ 0 & 0 \end{bmatrix} - \begin{bmatrix} J & 0 \\ 0 & I_{n_\infty} \end{bmatrix}, \begin{bmatrix} B_1 \\ B_2 \end{bmatrix}, \begin{bmatrix} C_1 & C_2 \end{bmatrix} \right).$$

Note that due to the assumptions, the nilpotent matrix N in the WeierstraSS canonical form is zero. Using this realization it holds

$$\lim_{\omega\to\infty} G(\mathrm{i}\omega) = -C_2 B_2.$$

We consider structured perturbations of the matrix pencil which lead to

$$\begin{aligned} \lambda \begin{bmatrix} I_{n_\mathrm{f}} & 0 \\ 0 & 0 \end{bmatrix} - \left(\begin{bmatrix} J & 0 \\ 0 & I_{n_\infty} \end{bmatrix} + \begin{bmatrix} B_1 \\ B_2 \end{bmatrix} \Delta \begin{bmatrix} C_1 & C_2 \end{bmatrix} \right) \\ = \lambda \begin{bmatrix} I_{n_\mathrm{f}} & 0 \\ 0 & 0 \end{bmatrix} - \begin{bmatrix} J + B_1\Delta C_1 & B_1\Delta C_2 \\ B_2\Delta C_1 & I_{n_\infty} + B_2\Delta C_2 \end{bmatrix}, \end{aligned}$$

where $\Delta \in \mathbb{C}^{m\times p}$. In [2, Theorem 3] it is shown that the perturbed transfer function is improper if and only if $I_{n_\infty} + B_2\Delta C_2$ is singular. Therefore we have to determine the value of

$$\begin{aligned} p_{\mathbb{C}} :&= \inf \left\{ \|\Delta\|_2 : I_{n_\infty} + B_2\Delta C_2 \text{ is singular with } \Delta \in \mathbb{C}^{m\times p} \right\} \\ &= \inf \left\{ \|\Delta\|_2 : -I_{n_\infty} + B_2\Delta C_2 \text{ is singular with } \Delta \in \mathbb{C}^{m\times p} \right\}. \end{aligned}$$

We consider the structured stability radius $r_{\mathbb{C}}(0, -I_{n_\infty}, B_2, C_2)$ of $-I_{n_\infty}$ with respect to B_2 and C_2. By employing [13, Proposition 2.1] we obtain

$$\begin{aligned} r_{\mathbb{C}}(0, -I_{n_\infty}, B_2, C_2) &= \frac{1}{\max\limits_{\omega\in\mathbb{R}} \sigma_{\max}(C_2((\mathrm{i}\omega+1)I_{n_\infty})^{-1}B_2)} \\ &= \frac{1}{\sigma_{\max}(C_2B_2)} \\ &= \frac{1}{\lim\limits_{\omega\to\infty} \sigma_{\max}(G(\mathrm{i}\omega))}. \end{aligned} \tag{3.1}$$

Since the maximum in (3.1) is attained at $\omega = 0$, we have $p_{\mathbb{C}} = r_{\mathbb{C}}(0, -I_{n_\infty}, B_2, C_2)$. This shows the assertion. ∎

PROPOSITION 3.2. *It holds*

$$r_{\mathbb{C}}(E,A,B,C) = \begin{cases} \frac{1}{\|G\|_{\mathcal{H}_\infty}} & \text{if } G \not\equiv 0, \\ \infty & \text{if } G \equiv 0. \end{cases} \tag{3.2}$$

Proof. The proof is similar to the corresponding one for state-space systems in [13]. First we analyze the case that the value of the $\mathcal{H}_\infty$-norm is attained at some finite $\omega \in \mathbb{R}$.

Assume that for some $\Delta \in \mathbb{C}^{m\times p}$, $0 \neq x \in \mathbb{C}^m$, and $\omega \in \mathbb{R}$ we have

$$(A + B\Delta C)x = \mathrm{i}\omega Ex,$$

or equivalently

$$x = (\mathrm{i}\omega E - A)^{-1}B\Delta Cx.$$

Since $G(s)$ is stable, we have $u := Cx \neq 0$, i.e.,

$$u = G(\mathrm{i}\omega)\Delta u. \tag{3.3}$$

If $G \equiv 0$ this leads to a contradiction and so $r^{\mathrm{f}}_{\mathbb{C}}(E, A, B, C) = \infty$, otherwise (3.3) implies $\|G(\mathrm{i}\omega)\|_2 \|\Delta\|_2 \geq 1$.

Now suppose that $\|G\|_{\mathcal{H}_\infty}$ is attained at ω_0, i.e., $\|G(\mathrm{i}\omega_0)\|_2 = \|G\|_{\mathcal{H}_\infty}$. Let

$$G(\mathrm{i}\omega_0) = \sum_{j=1}^{k} \sigma_j u_j v_j^H$$

be a singular value decomposition of $G(\mathrm{i}\omega_0)$ with $u_j \in \mathbb{C}^p$, $v_j \in \mathbb{C}^m$, $\|u_j\|_2 = \|v_j\|_2 = 1$, for $j = 1, \ldots, k := \min\{m, p\}$, and $\|G(\mathrm{i}\omega_0)\|_2 = \sigma_1 \geq \sigma_2 \geq \ldots \geq \sigma_k$. With $\Delta := \sigma_1^{-1} v_1 u_1^H$ it follows that

$$G(\mathrm{i}\omega_0)\Delta u_1 = C(\mathrm{i}\omega_0 E - A)^{-1}B\Delta u_1 = u_1.$$

Defining $x := (\mathrm{i}\omega_0 E - A)^{-1}B\Delta u_1$ leads to $Cx = u_1$ and hence $x \neq 0$. This yields

$$x := (\mathrm{i}\omega_0 E - A)^{-1}B\Delta Cx,$$

and consequently

$$(A + B\Delta C)\, x = \mathrm{i}\omega_0 Ex.$$

From

$$x^H \begin{bmatrix} \mathrm{i}\omega_0 E^T - (A + B\Delta C)^T & C^T \end{bmatrix} = \begin{bmatrix} 0 & x^H C^T \end{bmatrix} = \begin{bmatrix} 0 & u_1 \end{bmatrix},$$

with $u_1 \neq 0$, we conclude that $\mathrm{i}\omega_0$ is an observable pole of the perturbed transfer function

$$C\,(sE - (A + B\Delta C))^{-1}\, B.$$

Similarly we can prove controllability of $\mathrm{i}\omega_0$.

From that we conclude $\|\Delta\|_2 = \frac{1}{\|G\|_{\mathcal{H}_\infty}}$, where Δ is a perturbation of infimal norm such that $\Pi_{\mathrm{f}}(E, A + B\Delta C, B, C) \cap \mathrm{i}\mathbb{R} \neq \emptyset$.

This shows that $\|G\|_{\mathcal{H}_\infty} = \|G(\mathrm{i}\omega)\|_2$ for some $\omega \in \mathbb{R}$ if and only if $r_{\mathbb{C}}(E, A, B, C) = r^{\mathrm{f}}_{\mathbb{C}}(E, A, B, C)$. The case that the norm value is attained at infinity is covered by Lemma 3.1. ∎

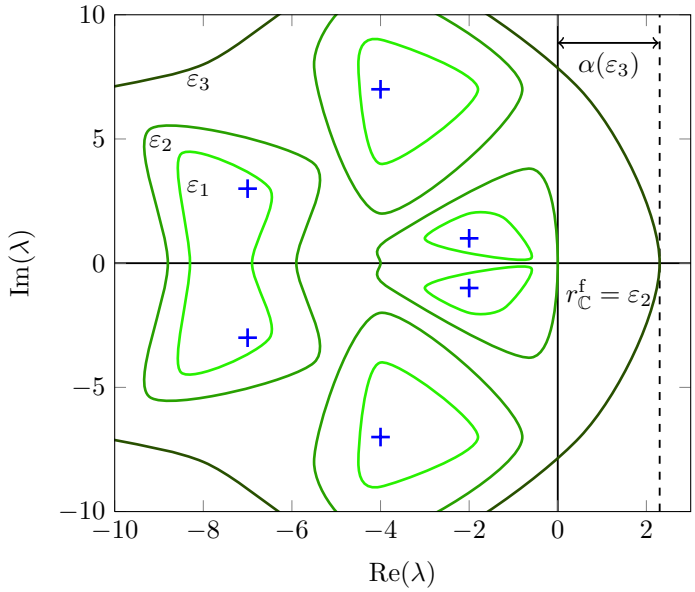

Fig. 3.1: Poles (blue crosses) and structured pseudospectra of a transfer function to different perturbation levels

For the remainder of the article we need the following definitions.

DEFINITION 3.3. *The* structured ε-pseudospectrum of the transfer function $G(s)$ *with respect to* B *and* C *is defined by*

$$\Pi_\varepsilon(E,A,B,C) = \{s \in \mathbb{C} : s \in \Pi_f(E, A + B\Delta C, B, C) \text{ for some } \Delta \in \mathbb{C}^{m\times p} \text{ with } \|\Delta\|_2 < \varepsilon\}.$$

Furthermore, the structured ε-pseudospectral abscissa *is given by*

$$\alpha_\varepsilon(E,A,B,C) := \max\{\operatorname{Re} s : s \in \Pi_\varepsilon(E,A,B,C)\}.$$

A graphical interpretation of the terms defined in Definition 3.3 is given in Figure 3.1.

From these definitions it is clear that $\alpha_{r^f_{\mathbb{C}}}(E,A,B,C) = 0$. So the main idea of our algorithm is to find the (unique) root of the function $\alpha(\varepsilon) := \alpha_\varepsilon(E,A,B,C)$. To get an efficient algorithm we need to evaluate $\alpha(\varepsilon)$ for different values of ε in a cheap way.

3.1. Computation of the Structured ε-Pseudospectral Abscissa. In this subsection we derive a fast algorithm for computing $\alpha(\varepsilon)$. The following fundamental results are generalizations of the corresponding ones in [20].

LEMMA 3.4. *Let* $s \in \mathbb{C}\backslash\Pi_f(E,A,B,C)$ *be given and* $\varepsilon > 0$. *Then the following statements are equivalent:*

(a) $s \in \Pi_\varepsilon(E,A,B,C)$.

(b) $\sigma_{\max}(G(s)) > \varepsilon^{-1}$.

(c) There exist vectors $u \in \mathbb{C}^m$ *and* $v \in \mathbb{C}^p$ *with* $\|u\|_2 < 1$ *and* $\|v\|_2 < 1$ *such that* $s \in \Pi_f\left(E, A + \varepsilon B u v^H C, B, C\right)$.

Proof. "(a)$\Longrightarrow$(b)": From $s \in \Pi_\varepsilon(E, A, B, C)$ it follows that there exist a matrix $\Delta \in \mathbb{C}^{m\times p}$ with $\|\Delta\|_2 < \varepsilon$ and a vector $y \in \mathbb{C}^n$ such that

$$(sE - (A + B\Delta C))\, y = 0.$$

This is equivalent to

$$(sE - A)\, y = B\Delta C y$$

and therefore

$$Cy = C\,(sE - A)^{-1}\, B\Delta C y.$$

Now we can estimate

$$\|Cy\|_2 \leq \left\| C\,(sE - A)^{-1}\, B \right\|_2 \|\Delta\|_2 \, \|Cy\|_2 \,,$$

and hence

$$\varepsilon^{-1} < \|\Delta\|_2^{-1} \leq \|G(s)\|_2 \,.$$

"(b)$\Longrightarrow$(c)": Let $\sigma_{\max}(G(s)) > \varepsilon^{-1}$. Define $\sigma := \sigma_{\max}(G(s))$ with corresponding singular vectors $u \in \mathbb{C}^m$, $v \in \mathbb{C}^p$ satisfying $\|u\|_2 = \|v\|_2 = 1$. Then

$$G(s)u = \sigma v, \quad v^H G(s) = \sigma u^H, \quad \sigma > \varepsilon^{-1}. \tag{3.4}$$

Multiplying the first equation of (3.4) by v^H from the left and by $v^H C$ from the right yields

$$v^H C(sE - A)^{-1} B u v^H C = \sigma v^H v v^H C = \sigma v^H C.$$

By setting $\tilde{v}^H := v^H C(sE - A)^{-1}$ we obtain

$$\tilde{v}^H B u v^H C = \sigma \tilde{v}^H (sE - A).$$

The vector $\tilde{v}^H \neq 0$ since $v^H C \neq 0$, otherwise $\sigma = 0$ which is excluded since $\varepsilon > 0$. Therefore $sE - \hat{A} := sE - \left(A + \sigma^{-1} B u v^H C\right)$ is singular. It remains to show that s is indeed a pole of the perturbed transfer function

$$C\left(sE - \hat{A}\right)^{-1} B,$$

i.e., we have to prove controllability and observability of s. Since $\tilde{v}$ is a left eigenvector of $sE - \hat{A}$ it holds

$$\tilde{v}^H \begin{bmatrix} sE - \hat{A} & B \end{bmatrix} = \begin{bmatrix} 0 & \tilde{v}^H B \end{bmatrix} = \begin{bmatrix} 0 & v^H C(sE - A)^{-1} B \end{bmatrix} = \begin{bmatrix} 0 & \sigma u^H \end{bmatrix}.$$

Since $\sigma u^H \neq 0$, s is a controllable eigenvalue. Observability can be proven in an analogous manner and is therefore omitted. This yields statement (c).

"(c)$\Longrightarrow$(a)": This statement is trivial since with $\Delta := \varepsilon u v^H$ we obtain $s \in \Pi_{\mathrm{f}}(E, A + B\Delta C, B, C)$. ∎

From Theorem 3.4 we can conclude that

$$\Pi_\varepsilon(E, A, B, C) = \Pi_{\mathrm{f}}(E, A, B, C) \cup \left\{ s \in \mathbb{C} : \sigma_{\max}\left(G(s)\right) > \varepsilon^{-1} \right\}$$

with boundary

$$\partial\Pi_\varepsilon(E,A,B,C) = \left\{ s \in \mathbb{C} : \sigma_{\max}\left(G(s)\right) = \varepsilon^{-1} \right\}. \tag{3.5}$$

In other words, also the rightmost structured pseudopole is arbitrarily close to the curve $\partial\Pi_\varepsilon(E,A,B,C)$. Thus, our strategy consists of computing a sequence of suitable structured rank-1 perturbed pencils $\lambda E - (A + \varepsilon B u v^H C)$ such that one of the perturbed eigenvalues converges to the rightmost structured pseudopole of $G(s)$. A similar technique has already been successfully applied to compute the pseudospectral abscissa of a matrix, see [12]. We need the following result for the first order perturbation theory of matrix pencils. By $\mathbb{C}[\lambda]^{n\times n}$ we denote the set of all polynomials in λ with coefficients in $\mathbb{C}^{n\times n}$.

LEMMA 3.5. *[25] Let $\lambda E - A \in \mathbb{C}[\lambda]^{n\times n}$ be a given matrix pencil and let x, $y \in \mathbb{C}^n$ be right and left eigenvectors corresponding to a simple finite eigenvalue $\lambda = \frac{y^H A x}{y^H E x}$. Let $\lambda E - (A + t B u v^H C)$ be a perturbed matrix pencil with eigenvalue $\tilde{\lambda}$. Then it holds*

$$\tilde{\lambda} = \lambda + t\frac{y^H B u v^H C x}{y^H E x} + \mathcal{O}\left(t^2\right).$$

Furthermore, Lemma 3.5 directly yields

$$\left.\frac{\mathrm{d}\tilde{\lambda}(t)}{\mathrm{d}t}\right|_{t=0} = \frac{y^H B u v^H C x}{y^H E x}.$$

Now, we describe how such rank-1 perturbations can be constructed in an optimal way. Therefore, let $\lambda E - A$ with a simple eigenvalue λ and corresponding right and left eigenvectors x, y with $y^H E x > 0$ be given. Furthermore let $u \in \mathbb{C}^m$ and $v \in \mathbb{C}^p$ with $\|u\|_2 = \|v\|_2 = 1$ be given vectors. Then, it holds

$$\begin{aligned} \mathrm{Re}\left(\left.\frac{\mathrm{d}\tilde{\lambda}(t)}{\mathrm{d}t}\right|_{t=0} \right) &= \frac{\mathrm{Re}\left(y^H B u v^H C x\right)}{y^H E x} \\ &\leq \frac{\left\|y^H B\right\|_2 \|Cx\|_2}{y^H E x}. \end{aligned} \tag{3.6}$$

Equality in (3.6) holds for $u = \frac{B^H y}{\|B^H y\|_2}$, $v = \frac{Cx}{\|Cx\|_2}$. Hence, local maximal growth in $\mathrm{Re}\left(\tilde{\lambda}(t)\right)$ as t increases from 0 is achieved for this choice of u and v. In this way we generate the initial perturbation. Next we consider subsequent perturbations. Let therefore $\lambda E - \hat{A} := \lambda E - (A + \varepsilon B \hat{u} \hat{v}^H C)$ with a simple eigenvalue $\hat{\lambda}$ and associated right and left eigenvectors $\hat{x}$, $\hat{y}$ with $\hat{y}^H E \hat{x} > 0$ be the perturbed matrix pencil. Let in addition vectors $u \in \mathbb{C}^m$, $v \in \mathbb{C}^p$ with $\|u\|_2 = \|v\|_2 = 1$ be given. We consider the family of perturbations of the matrix pencil $\lambda E - \hat{A}$ of the form

$$\lambda E - \left(\hat{A} + tB\left(u v^H - \hat{u}\hat{v}^H\right) C \right),$$

which are structured ε-norm rank-1 perturbations of $\lambda E - A$ for $t = 0$ and $t = \varepsilon$. For the perturbed eigenvalue, for simplicity called again $\tilde{\lambda}$, we obtain

$$\begin{aligned} \mathrm{Re}\left(\left.\frac{\mathrm{d}\tilde{\lambda}(t)}{\mathrm{d}t}\right|_{t=0} \right) &= \frac{\mathrm{Re}\left(\hat{y}^H B\left(u v^H - \hat{u}\hat{v}^H\right) C \hat{x}\right)}{\hat{y}^H E \hat{x}} \\ &\geq \frac{\left\|\hat{y}^H B\right\|_2 \|C\hat{x}\|_2 - \mathrm{Re}\left(\hat{y}^H B \hat{u}\hat{v}^H C \hat{x}\right)}{\hat{y}^H E \hat{x}} \\ &\geq 0. \end{aligned} \tag{3.7}$$

Similar as above, equality in (3.7) holds for $u = \frac{B^H \hat{y}}{\|B^H \hat{y}\|_2}$, $v = \frac{C\hat{x}}{\|C\hat{x}\|_2}$. So, the basic algorithm consists of successively choosing an eigenvalue and constructing the perturbations described above by using the corresponding eigenvectors. However, an important question is how to actually choose these eigenvalues. This will be discussed in the next subsection.

3.2. Choice of the Eigenvalues. Recall, that we want to construct structured ε-norm rank-1 perturbations of the pencil $\lambda E - A$ such that one of the perturbed eigenvalues converges to the rightmost structured ε-pseudopole of the corresponding transfer function $G(s)$. Intuitively, in each step one would choose the rightmost eigenvalue of the perturbed pencil to construct the next perturbation. However, that might not be a good choice. Note, that the perturbability of an eigenvalue λ with right and left eigenvectors x and y highly depends on $\left\|B^H y\right\|_2$ and $\|Cx\|_2$. If these values are small, no large perturbation is possible. We recall, that these values are strongly related to the controllability and observability concepts introduced in Section 1. Roughly speaking, the "larger" $\left\|B^H y\right\|_2$ is, the "larger" is the distance of the system to uncontrollability at λ. So, large values of $\left\|B^H y\right\|_2$ indicate a good controllability at λ. Similar considerations can also be made for observability.

Consequently, for our algorithm we look for eigenvalues that have both sufficiently large real part and a high controllability and observability. An algorithm which unites both concepts and can compute the desired eigenvalues is the *(subspace accelerated MIMO) dominant pole algorithm (SAMDP)*, introduced by Rommes and Martins [21–24]. The algorithm has actually been designed to find the poles which have the highest influence on the frequency response of the transfer function $G(s)$. Assume that $\lambda E - A$ has only simple eigenvalues λ_k with left and right eigenvectors y_k and x_k, normalized such that $y_k^H E x_k = 1$. Then

$$G(s) = \sum_{k=1}^{n} \frac{R_k}{s - \lambda_k} + R_\infty \tag{3.8}$$

with the *residues*

$$R_k = C x_k y_k^H B, \text{ and } R_\infty = \lim_{\omega \to \infty} G(\mathrm{i}\omega).$$

Then, $\|R_k\|_2 = \|Cx_k\|_2 \left\|B^H y_k\right\|_2$ is a measure for simultaneous controllability and observability of λ_k. We observe that if λ_j is close to the imaginary axis and $\|R_j\|_2$ is large, then for $\omega \approx \mathrm{Im}(\lambda_j)$ it holds

$$G(\mathrm{i}\omega) \approx \frac{R_j}{-\mathrm{Re}(\lambda_j)} + \sum_{\substack{k=1 \\ k \neq j}}^{n} \frac{R_k}{\mathrm{i}\omega - \lambda_k} + R_\infty,$$

and therefore $\|G(\mathrm{i}\omega)\|_2$ is large, too. These considerations give the motivation for the following definition. We call an eigenvalue $\lambda_j \in \Lambda(E, A)$ *dominant pole* of $G(s)$, if

$$\frac{\|R_k\|_2}{|\mathrm{Re}(\lambda_k)|} < \frac{\|R_j\|_2}{|\mathrm{Re}(\lambda_j)|}, \quad k = 1, \ldots, n, \quad k \neq j. \tag{3.9}$$

The most dominant poles can be determined by SAMDP and are essentially what we are looking for. However, we also deal with positive structured pseudospectral abscissae. By using the definition (3.9), the eigenvalues tend to loose dominance

as soon as they have crossed the imaginary axis into the right half-plane. Then, in subsequent iterations eigenvalues in the left half-plane tend to be determined as most dominant. This is of course an undesired behavior since this could lead to convergence problems when the rightmost pseudoeigenvalue is "far" in the right half-plane. Therefore we use an alternative dominance measure which does not have that drawback. We call an eigenvalue $\lambda_j \in \Lambda_{\mathrm{f}}(E, A)$ *exponentially dominant pole* of $G(s)$, if

$$\|R_k\|_2 \exp(\beta \operatorname{Re}(\lambda_k)) \;<\; \|R_j\|_2 \exp(\beta \operatorname{Re}(\lambda_j)), \quad k \;=\; 1, \ldots, n, \quad k \;\neq\; j. \quad (3.10)$$

The parameter β is a weighting factor which defines the trade-off between the influence of the residue and real part of the eigenvalues. In our numerical experiments it turned out that $\beta = 100$ is a good choice for many examples (high weight on the real part). Since SAMDP delivers the poles which have the highest influence on the frequency response of a system and due to the relation (3.2), we can determine very good initial estimates for $r^{\mathrm{f}}_{\mathbb{C}}(E, A, B, C)$. We compute some of the dominant poles λ_k, $k = 1, \ldots, \ell$ and determine an estimate $r^{\mathrm{est}}_{\mathbb{C}}(E, A, B, C)$ as

$$r^{\mathrm{est}}_{\mathbb{C}}(E, A, B, C) = 1/ \max_{1 \le k \le \ell} \sigma_{\max}\left(G\left(\mathrm{i}\omega_k\right)\right) \quad (3.11)$$

with $\omega_k = \operatorname{Im}(\lambda_k)$, $k = 1, \ldots, \ell$.

3.3. Algorithmic Details. In this subsection we present some pseudocode of the algorithms that have been derived. Algorithm 1 summarizes the procedure for the computation of the structured ε-pseudospectral abscissa. In our implementation of the algorithm we use estimates of the eigenvectors x and y that are used to construct the optimal perturbation. This is possible since we can take the eigenvectors returned by the previous $\alpha(\varepsilon)$-evaluations of the root-finding algorithm. This accelerates the computation drastically since in the final root-finding steps the eigenvectors also converge to x and y.

We mention the drawback that the algorithm not necessarily converges to the globally rightmost value on the boundary of the ε-pseudospectrum $\partial\Pi_\varepsilon(E, A, B, C)$ in (3.5). Mostly it does but in some rare situations the algorithm converges only to a local maximizer. This especially happens in the first iteration of the root-finding algorithm when no good estimates of the optimal eigenvectors are available. Therefore, sometimes one has to try several dominant poles to find the global maximizer in the beginning. To find the root of $\alpha(\varepsilon)$ we use a simple secant method [18], summarized by Algorithm 2 which has a superlinear convergence with convergence rate $\frac{1+\sqrt{5}}{2} \approx 1.618$. As the numerical examples show, we only need very few (3-5) iterations of this method in most cases to find the root with a sufficient accuracy. When computing the dominant poles of the system we already obtain a very good estimate of $r^{\mathrm{est}}_{\mathbb{C}}(E, A, B, C)$ as in (3.11). This value is used as first initial value of Algorithm 2. The other one is obtained by multiplying the estimate $r^{\mathrm{est}}_{\mathbb{C}}(E, A, B, C)$ by a factor γ. For many examples, $r^{\mathrm{est}}_{\mathbb{C}}(E, A, B, C)$ is so good, that we can take a rather large value of γ such as 0.8. Furthermore, we estimate $\lim_{\omega\to\infty} G(\mathrm{i}\omega)$ by evaluating $G(\mathrm{i}\omega)$ for a sufficiently large ω. The largest singular value of $G(\mathrm{i}\omega)$ will converge quickly due to fact that for large ω there are no close finite poles which can introduce peaks. We can give the following upper bound using the residue representation of the transfer

Algorithm 1 Computation of the structured pseudospectral abscissa

Input: System $\Sigma = (\lambda E - A, B, C)$, perturbation level ε, tolerance on relative change τ.

Output: $\alpha_\varepsilon(E, A, B, C)$.

1: Compute the exponentially dominant pole λ_0 of $(\lambda E - A, B, C)$ with left and right eigenvectors y_0 and x_0.
2: Compute the perturbation $\hat{A} = A + \varepsilon \frac{BB^H y_0 x_0^H C^H C}{\|B^H y_0\|_2 \|C x_0\|_2}$.
3: **for** $j = 1, 2, \ldots$ **do**
4: Compute the exponentially dominant pole λ_j of $(\lambda E - \hat{A}, B, C)$ with left and right eigenvectors y_j and x_j.
5: **if** $|\mathrm{Re}\,(\lambda_j) - \mathrm{Re}\,(\lambda_{j-1})| < \tau\,|\mathrm{Re}\,(\lambda_j)|$ **then**
6: Set $k = j$.
7: Break.
8: **end if**
9: Compute the perturbation $\hat{A} = A + \varepsilon \frac{BB^H y_j x_j^H C^H C}{\|B^H y_j\|_2 \|C x_j\|_2}$.
10: **end for**
11: $\alpha_\varepsilon(E, A, B, C) = \mathrm{Re}\,(\lambda_k)$.

Algorithm 2 Computation of the structured complex stability radius

Input: System $\Sigma = (\lambda E - A, B, C)$ with transfer function $G(s)$, control parameter $0 < \gamma < 1$.

Output: $\|G\|_{\mathcal{H}_\infty}$.

1: Set $\varepsilon_1 = r_{\mathbb{C}}^{\mathrm{est}}(E, A, B, C)$ as in (3.11).
2: Set $\varepsilon_2 = \gamma \varepsilon_1$.
3: **for** $j = 1, 2, \ldots, k$ **do**
4: Compute $\varepsilon_{j+2} = \varepsilon_{j+1} - \frac{\varepsilon_{j+1} - \varepsilon_j}{\alpha(\varepsilon_{j+1}) - \alpha(\varepsilon_j)} \alpha(\varepsilon_{j+1})$.
5: **end for**
6: Compute $r_{\mathbb{C}}^{\infty}(E, A, B, C) = 1 / \lim_{\omega \to \infty} \sigma_{\max}(G(\mathrm{i}\omega))$.
7: Set $\|G\|_{\mathcal{H}_\infty} = \max\left\{\varepsilon_k^{-1}, r_{\mathbb{C}}^{\infty}(E, A, B, C)^{-1}\right\}$.

function (3.8) with $\lambda_k = \nu_k + \mathrm{i}\omega_k,\ k = 1, \ldots, n$:

$$\begin{aligned} \|G(\mathrm{i}\omega)\|_2 &= \left\| \sum_{k=1}^{n} \frac{R_k}{\mathrm{i}\omega - \mathrm{i}\omega_k - \nu_k} + R_\infty \right\|_2 \\ &\leq \sum_{k=1}^{n} \frac{\|R_k\|_2}{|\mathrm{i}\omega - \mathrm{i}\omega_k - \nu_k|} + \|R_\infty\|_2 . \end{aligned} \tag{3.12}$$

For $\omega \gg \max_{1 \leq k \leq n} \omega_k$ we can neglect the real parts of the denominators $\nu_k,\ k = 1, \ldots, n$. Since usually there are only very few dominant poles, we can control the desired accuracy by, e.g., choosing ω such that for the most dominant pole λ_j we have

$$\frac{\|R_j\|_2}{|\omega - \omega_j|} \leq \eta$$

for some small $\eta > 0$.

4. Numerical Results.

4.1. Test Setup. In this section be present some numerical results of our implementations. The tests have been performed on a 2.6.32-23-generic-pae Ubuntu machine with Intel® Core™2 Duo CPU with 3.00GHz and 2GB RAM. The algorithms have been implemented and tested in MATLAB 7.11.0.584 (R2010b). To compute the (exponentially) dominant poles we use a (modified) implementation of Rommes' MATLAB codes*. The data for the numerical examples was taken from [9, 11, 16, 22] and it can also be downloaded from Rommes' website or from the NICONET page†. In the dominance measure in (3.10) we use $\beta = 100$. The tolerance on the relative change of the iterates in Algorithm 1 is set to $\tau = 10^{-3}$. We also abort the iteration when the iterates are smaller than $1000\mathbf{u}$, where $\mathbf{u}$ denotes the machine precision, or when the iterates start to cycle which typically happens when they are approaching zero. In Algorithm 2 we set $\gamma = 0.8$. We abort this iteration when the relative change of the iterates is below 10^{-6}, i.e., if $\left|1 - \frac{\varepsilon_k}{\varepsilon_{k+1}}\right| < 10^{-6}$. To obtain $r^{\text{est}}_{\mathbb{C}}(E, A, B, C)$ we compute 20 dominant poles using the original version of SAMDP. For every further outer iteration we compute only 5 dominant poles using the modified algorithm with the exponential dominance measure.

4.2. Test Results. In Table 4.1 we summarize the results of 34 numerical tests. The first 13 examples are standard or generalized state space systems whereas the other 21 ones are descriptor systems (with singular E). With n_{outer} we denote the number of outer iterations, i.e., the number of steps needed by Algorithm 2 to find the root. With n_{inner} we refer to the total number of inner iterations, i.e., the total number of steps needed by Algorithm 1.

For all but one test (`peec`), the correct value of $\|G\|_{\mathcal{H}_\infty}$ was found. In 29 tests the first outer iteration returned a positive value. However, for 3 tests (`M10PI_n1`, `M10PI_n`, `bips07_1693`), a negative value was returned and therefore we had to try more dominant poles (one for each `M10PI_n1`, `M10PI_n` and four for `bips07_1693`) to converge to the correct initial value. In one test (`iss`), $r^{\text{est}}_{\mathbb{C}}(E, A, B, C)$ underestimated $r^{\text{f}}_{\mathbb{C}}(E, A, B, C)$ due to inaccuracies when evaluating the largest singular values of $G(\mathrm{i}\omega)$. Then, for this example a correct negative structured pseudospectral was returned. Also the second initial guess was negative. However, the secant method does not require the initial guesses to enclose the root and therefore a correct norm value was returned. Note also that the convergence speed of the algorithm highly depends on the properties of the examples, e.g., for `bips07_1998` the convergence was significantly slower than for the rest in the `bips07` group, although they are comparable in size.

For a more detailed impression of the behavior of the algorithm, Table 4.2 summarizes the convergence history for the `M20PI_n` and the `bips07_2476` examples, listing each intermediate iterate for each iteration of the root-finding algorithm.

Finally, in Figure 4.1 the transfer functions for the `M20PI_n` and the `bips07_2476` examples are evaluated on the imaginary axis including the computed $\mathcal{H}_\infty$-norm. We see that for `M20PI_n`, the algorithm computes the correct value, even though there are lots of close-by peaks of similar height.

4.3. Limitations of the Method. In this subsection we explain limitations of our method. We have already mentioned that the algorithm fails for the `peec` example. We plotted the transfer function of this example in Figure 4.2, once in the interval $(0, 10)$ and once for the interval $(5.2, 5.5)$ where the maximum peak is

*`http://sites.google.com/site/rommes/software`

†`http://www.icm.tu-bs.de/NICONET/benchmodred.html`

Table 4.1: Numerical results for 34 test examples

#	example	n	m	p	$\|G\|_{\mathcal{H}_\infty}$	$\alpha_{r_{\mathbb{C}}^{\mathrm{f}}}(E,A,B,C)$	n_{outer}	n_{inner}	time in s
1	build	48	1	1	5.27633e-03	7.7500e-13	4	17	2.07
2	pde	84	1	1	1.08358e+01	2.0964e-15	2	6	2.25
3	CDplayer	120	2	2	2.31982e+06	8.6537e-16	3	9	3.10
4	iss	270	3	3	1.15885e-01	1.4302e-16	7	23	17.49
5	beam	348	1	1	4.55487e+03	-1.1269e-12	3	10	48.53
6	S10PI_n1	528	1	1	3.97454e+00	-5.5702e-13	4	14	3.16
7	S20PI_n1	1028	1	1	3.44317e+00	8.0050e-12	4	15	5.19
8	S40PI_n1	2028	1	1	3.34732e+00	1.3020e-10	4	18	9.33
9	S80PI_n1	4028	1	1	3.37016e+00	-1.1361e-12	4	14	15.76
10	M10PI_n1	528	3	3	4.05662e+00	1.9585e-13	5	18	4.93
11	M20PI_n1	1028	3	3	3.87260e+00	1.3484e-12	4	14	5.71
12	M40PI_n1	2028	3	3	3.81767e+00	1.1625e-12	4	15	9.25
13	M80PI_n1	4028	3	3	3.80375e+00	1.3691e-12	4	14	16.18
14	peec	480	1	1	3.79802e-02	6.19760e-11	5	21	22.07
15	S10PI_n	682	1	1	3.97454e+00	1.1684e-12	4	14	3.93
16	S20PI_n	1182	1	1	3.44317e+00	7.7902e-12	4	15	5.42
17	S40PI_n	2182	1	1	3.34732e+00	1.3191e-10	4	18	10.01
18	S80PI_n	4182	1	1	3.37016e+00	-6.3183e-13	4	14	15.96
19	M10PI_n	682	3	3	4.05662e+00	9.2788e-13	5	18	5.50
20	M20PI_n	1182	3	3	3.87260e+00	7.0597e-13	4	14	6.37
21	M40PI_n	2182	3	3	3.81767e+00	3.0692e-13	4	14	9.26
22	M80PI_n	4182	3	3	3.80375e+00	-2.0151e-13	4	14	18.16
23	bips98_606	7135	4	4	2.01956e+02	2.4138e-12	4	16	44.30
24	bips98_1142	9735	4	4	1.60427e+02	-5.8626e-11	4	28	88.51
25	bips98_1450	11305	4	4	1.97389e+02	4.5911e-13	5	26	97.61
26	bips07_1693	13275	4	4	2.04168e+02	3.9603e-14	9	52	191.83
27	bips07_1998	15066	4	4	1.97064e+02	7.2725e-14	4	28	140.63
28	bips07_2476	16861	4	4	1.89579e+02	1.2551e-11	4	57	282.32
29	bips07_3078	21128	4	4	2.09445e+02	1.0384e-13	5	19	145.20
30	nopss_11k	11685	1	1	8.52671e-02	-6.4347e-14	6	42	127.49
31	xingo_afonso_itaipu	13250	1	1	4.05605e+00	-3.0780e-14	3	9	47.60
32	mimo8x8_system	13309	8	8	5.34292e-02	3.4737e-13	4	24	107.60
33	mimo28x28_system	13251	28	28	1.18618e-01	1.2423e-13	3	11	104.14
34	mimo46x46_system	13250	46	46	2.05631e+02	-4.4721e-14	3	11	157.40

Table 4.2: Convergence history for the `M20PI_n` example

	k			
	1	2	3	4
$\mathrm{Re}(\lambda_{\mathrm{dom}})$	-6.7945e-02	-6.0215e+00	-3.7397e-04	3.6361e-11
	2.3140e-03	-6.0212e+00	-3.4533e-05	3.9060e-11
	3.0285e-03	—	-3.2591e-05	3.8927e-11
	3.0355e-03	—	-3.2572e-05	—
	3.0356e-03	—	—	—
ε_k	2.582502e-01	2.066001e-01	2.582241e-01	2.582244e-01

Table 4.3: Convergence history for the `bips07_2476` example

	k			
	1	2	3	4
$\mathrm{Re}(\lambda_{\mathrm{dom}})$	-8.1617e-02	-2.4866e-01	-2.1375e-02	5.7642e-09
	-9.6637e-03	-2.1398e-01	-4.5199e-03	6.9168e-09
	-2.6717e-03	-2.0953e-01	-1.5636e-03	7.5480e-09
	-9.8184e-04	-2.0946e-01	-6.5744e-04	7.8936e-09
	-3.9561e-04	—	-3.0633e-04	8.0829e-09
	-1.5362e-04	—	-1.5235e-04	8.1865e-09
	-4.3525e-05	—	-7.9712e-05	8.2433e-09
	9.6185e-06	—	-4.3824e-05	8.2744e-09
	3.6273e-05	—	-2.5544e-05	8.2914e-09
	4.9989e-05	—	-1.6037e-05	8.3007e-09
	5.7173e-05	—	-1.1022e-05	8.3059e-09
	6.0984e-05	—	-8.3478e-06	—
	6.3022e-05	—	-6.9119e-06	—
	6.4120e-05	—	-6.1368e-06	—
	6.4714e-05	—	-5.7167e-06	—
	6.5036e-05	—	-5.4883e-06	—
	6.5211e-05	—	-5.3640e-06	—
	6.5307e-05	—	-5.2962e-06	—
	6.5359e-05	—	-5.2591e-06	—
	—	—	-5.2389e-06	—
	—	—	-5.2278e-06	—
	—	—	-5.2218e-06	—
	—	—	-5.2185e-06	—
ε_k	5.275154e-03	4.220124e-03	5.274825e-03	5.274850e-03

located. First of all we see, the transfer function has lots of peaks which is due to the high amount of poles close to the imaginary axis. We plotted the eigenvalues of the corresponding pencil $\lambda E - A$ in Figure 4.3, together with the ten most dominant poles. It is very hard for SAMDP to find the most dominant pole. In fact, if we only compute 20 dominant poles, the actually most dominant one is not found. This is only the case if we increase the number of wanted poles up to 30. Another problem is that the maximum peak is extremely thin and spiky. We do not even see it with

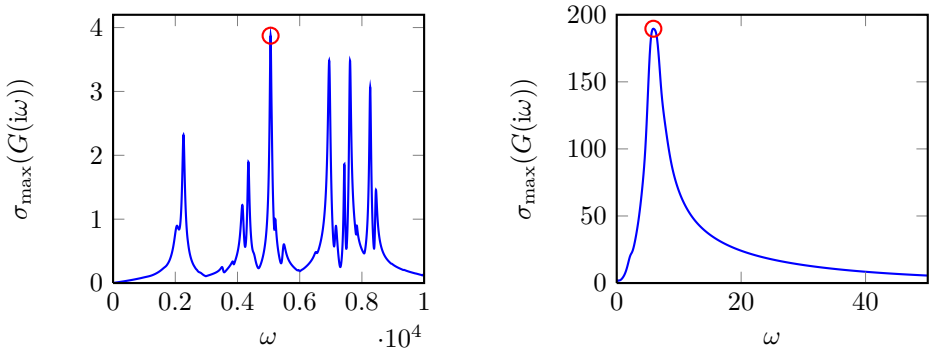

(a) `M20PI_n` (b) `bips07_2476`

Fig. 4.1: Transfer function plots for the `M20PI_n` and `bips07_2476` test examples with computed $\mathcal{H}_\infty$-norm (red circle)

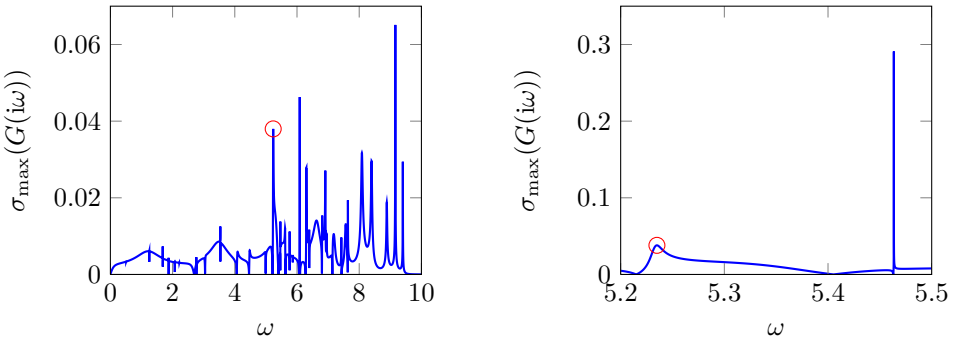

(a) Interval $(0, 10)$ (b) Zoom into the interval $(5.2, 5.5)$

Fig. 4.2: Transfer function plots for the `peec` example

the resolution used for plotting Figure 4.2(a). To find it we would actually need very good approximations the eigenvectors which are needed to construct the optimal rank-1 perturbation. However, our eigenvector approximations are not that good and therefore we only find a close-by peak. However, we can check if the computed norm value is larger than the 2-norms of the transfer function evaluated at the test frequencies. For this example, the test is not satisfied and therefore we can at least return an error indicator.

Other critical problems are those where $\lambda E - A$ has only real eigenvalues. For this kind of examples we observed an extremely slow convergence of SAMDP. Furthermore, it might happen that the most dominant poles are not the rightmost ones. Then, Algorithm 1 might only converge to inner eigenvalues of the perturbed pencils which forces the iteration to fail. Typically, the circuit examples from the `MNA` group of [9] are of this kind. However, for these problems, the $\mathcal{H}_\infty$-norm is attained at zero, i.e., $\|G\|_{\mathcal{H}_\infty} = \|G(0)\|_2$, see [19].

5. Conclusions and Future Research Perspectives. In this paper we have introduced a new iterative scheme for computing the $\mathcal{H}_\infty$-norm of a transfer function.

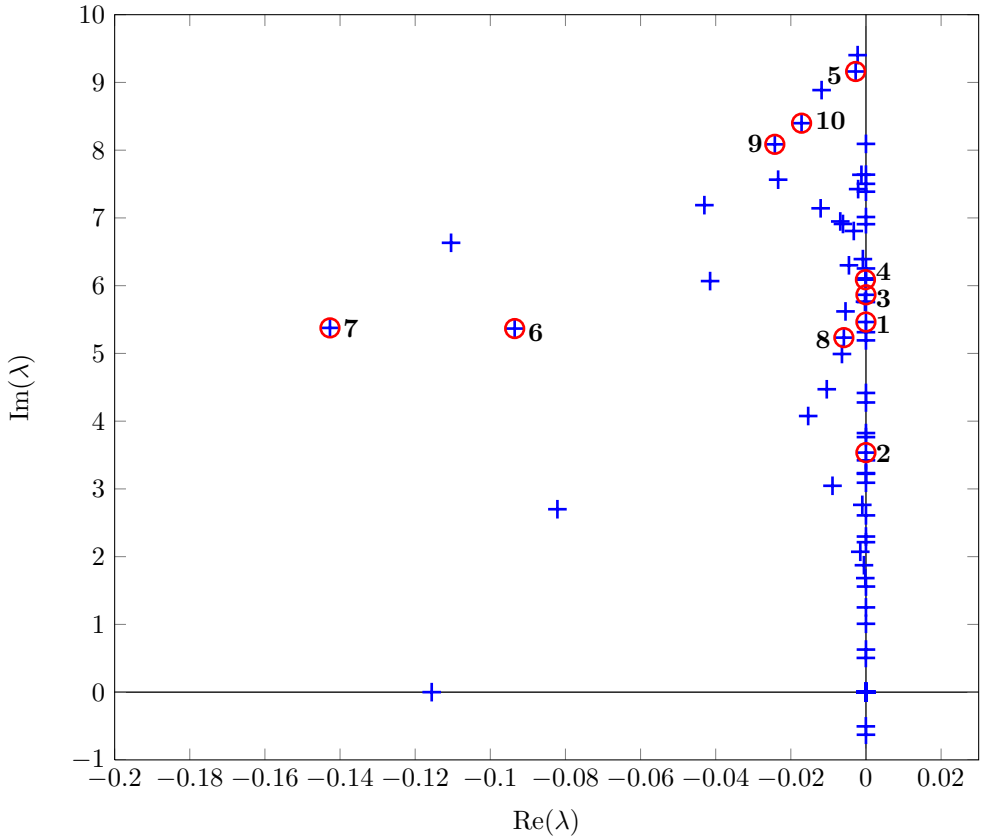

Fig. 4.3: Eigenvalues of $\lambda E - A$ for the `peec` example (blue pluses) and the 10 most dominant poles (red circles)

This routine uses the relationship between the $\mathcal{H}_\infty$-norm the structured complex stability radius of a matrix or a pencil. Based on the method introduced in [12], the algorithm computes a sequence of structured pseudospectral abscissae. This is done by computing an optimal rank-1 perturbation of the system such that one of the eigenvalues of the perturbed matrix or pencil converges to the rightmost structured pseudopole of the transfer function. This algorithm can be seen as a basis to solve certain related problems. Open questions are concerned with the computation of unstructured stability radii. Another interesting problem is the computation of *real* stability radii where the perturbation matrix is only allowed to be real. Finally, we also mention the passivity radius of a dynamical system which might also be put into this framework.

Acknowledgment. The authors thank Volker Mehrmann from TU Berlin for pointing at the difficulties arising if the perturbations make the transfer functions improper.

REFERENCES

[1] P. Benner, R. Byers, V. Mehrmann, and H. Xu. Numerical computation of deflating subspaces of embedded Hamiltonian pencils. Technical report, Chemnitz University of Technology, Department of Mathematics, Germany, June 1999. SFB393-Preprint 99-15.

[2] P. Benner, V. Sima, and M. Voigt. $\mathcal{L}_\infty$-norm computation for continuous-time descriptor systems using structured matrix pencils. *IEEE Trans. Automat. Control*, 57(1):233–238, Jan. 2012.

[3] S. Boyd and V. Balakrishnan. A regularity result for the singular values of a transfer matrix and a quadratically convergent algorithm for computing its L_∞-norm. *Syst. Control Lett.*, 15(1):1–7, 1990.

[4] S. Boyd, V. Balakrishnan, and P. Kabamba. A bisection method for computing the H_∞ norm of a transfer matrix and related problems. *Mathematics of Control, Signals, and Systems*, 2(3):207–219, September 1989.

[5] N. A. Bruinsma and M. Steinbuch. A fast algorithm to compute the H_∞-norm of a transfer function matrix. *Syst. Control Lett.*, 14(4):287–293, 1990.

[6] R. Byers. A bisection method for measuring the distance of a stable matrix to the unstable matrices. *SIAM J. Sci. Stat. Comput.*, 9:875–881, September 1988.

[7] Y. Chahlaoui, K. Gallivan, and P. Van Dooren. $\mathcal{H}_\infty$-norm calculations of large sparse systems. In *Proceedings International Symposium Math. Th. Netw. Syst.*, Leuven, Belgium, 2004.

[8] Y. Chahlaoui, K. Gallivan, and P. Van Dooren. Calculating the $\mathcal{H}_\infty$ norm of a large sparse system via Chandrasekhar iterations and extrapolation. In *ESAIM Proceedings*, volume 20, pages 83–92, Rabat, Algeria, October 2007.

[9] Y. Chahlaoui and P. Van Dooren. A collection of benchmark examples for model reduction of linear time invariant dynamical systems. Technical report, February 2002. SLICOT Working Note 2002–2.

[10] L. Dai. *Singular Control Systems*, volume 118 of *Lecture Notes in Control and Information Sciences*. Springer-Verlag, Heidelberg, 1989.

[11] F. Freitas, J. Rommes, and N. Martins. Gramian-based reduction method applied to large sparse power system descriptor models. *IEEE Trans. Power Syst.*, 23(3):1258–1270, August 2008.

[12] N. Guglielmi and M. L. Overton. Fast algorithms for the approximation of the pseudospectral abscissa and pseudospectral radius of a matrix. *SIAM J. Matrix Anal. Appl.*, 32(4):1166–1192, 2011.

[13] D. Hinrichsen and A. J. Pritchard. Stability radius for structured perturbations and the algebraic Riccati equation. *Syst. Control Lett.*, 8:105–113, August 1986.

[14] D. Hinrichsen and A. J. Pritchard. *Real and Complex Stability Radii: A Survey*, volume 6 of *Progress in Systems and Control Theory*, pages 119–162. Birkhäuser, Boston, 1990.

[15] P. Kunkel and V. Mehrmann. *Differential-Algebraic Equations - Analysis and Numerical Solution*. Textbooks in Mathematics. European Mathematical Society, 2006.

[16] N. Martins, P. C. Pellanda, and J. Rommes. Computation of transfer function dominant zeros with applications to oscillation damping control of large power systems. *IEEE Trans. Power Syst.*, 22(4):1657–1664, November 2007.

[17] V. Mehrmann, C. Schröder, and V. Simoncini. An implicitly-restarted Krylov subspace method for real symmetric/skew-symmetric eigenproblems. *Lin. Alg. Appl.*, 2009. in press.

[18] W. H. Press, B. P. Flannery, S. A. Teukolsky, and W. T. Vetterling. Secant method, false position method and Ridders' method. In *Numerical Recipes in FORTRAN: The Art of Scientific Computing*, chapter 9.2, pages 347–352. Cambridge University Press, Cambridge, England, 2 edition, 1992.

[19] T. Reis and T. Stykel. Lyapunov balancing for passivity-preserving model reduction of RC circuits. *SIAM J. Appl. Dyn. Syst.*, 10(1):1 – 34, January 2011.

[20] K. S. Riedel. Generalized epsilon-pseudospectra. *SIAM J. Numer. Anal.*, 31:1219–1225, 1994.

[21] J. Rommes. Arnoldi and Jacobi-Davidson methods for generalized eigenvalue problems $Ax = \lambda Bx$ with singular B. *Math. Comp.*, 77:995–1015, 2008.

[22] J. Rommes and N. Martins. Efficient computation of multivariate transfer function dominant poles using subspace acceleration. *IEEE Trans. Power Syst.*, 21(4):1471–1483, November 2006.

[23] J. Rommes and N. Martins. Efficient computation of transfer function dominant poles using subspace acceleration. *IEEE Trans. Power Syst.*, 21(3):1218–1226, August 2006.

[24] J. Rommes and G. L. G. Sleijpen. Convergence of the dominant pole algorithm and Rayleigh quotient iteration. *SIAM J. Matrix Anal. Appl.*, 30(1):346–363, February 2008.

[25] G. W. Stewart and J.-G. Sun. *Matrix Perturbation Theory*. Computer science and scientific computing. Academic Press, 1990.

[26] K. Zhou and J. D. Doyle. *Essentials of Robust Control*. Prentice Hall, 1st edition, 1998.